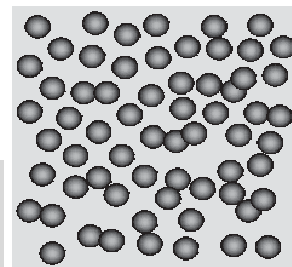


DOI: 10.1002/adma.200600527

# New Directions for Low-Dimensional Thermoelectric Materials\*\*

By Mildred S. Dresselhaus,\* Gang Chen, Ming Y. Tang, Ronggui Yang, Hohyun Lee, Dezhi Wang, Zhifeng Ren, Jean-Pierre Fleurial, and Pawan Gogna



*Many of the recent advances in enhancing the thermoelectric figure of merit are linked to nanoscale phenomena found both in bulk samples containing nanoscale constituents and in nanoscale samples themselves.*

*Prior theoretical and experimental proof-of-principle studies on quantum-well superlattice and quantum-wire samples have now evolved into studies on bulk samples containing nanostructured constituents prepared by chemical or physical approaches. In this Review, nanostructural composites are shown to exhibit nanostructures and properties that show promise for thermoelectric applications, thus bringing together low-dimensional and bulk materials for thermoelectric applications. Particular emphasis is given in this Review to the ability to achieve 1) a simultaneous increase in the power factor and a decrease in the thermal conductivity in the same nanocomposite sample and for transport in the same direction and 2) lower values of the thermal conductivity in these nanocomposites as compared to alloy samples of the same chemical composition. The outlook for future research directions for nanocomposite thermoelectric materials is also discussed.*

## 1. Introduction

Providing a sustainable supply of energy to the world's population will become a major societal problem for the 21st

century as fossil fuel supplies decrease and world demand increases. Thermoelectric phenomena, which involve the conversion between thermal and electrical energy, and provide a method for heating and cooling materials, are expected to play an increasingly important role in meeting the energy challenge of the future. Therefore we can expect an increasing emphasis on the development of advanced thermoelectric materials as promising approaches are demonstrated, both at the proof-of-principle level and at the scale-up level. In this article, we review the present status of the newly emerging field of low-dimensional thermoelectricity, enabled by materials nanoscience and nanotechnology.

The field of thermoelectrics advanced rapidly in the 1950s when the basic science of thermoelectric materials became well established, the important role of heavily doped semiconductors as good thermoelectric materials became accepted, and the thermoelectric material  $\text{Bi}_2\text{Te}_3$  was developed for commercialization, thus launching the thermoelectrics indus-

[\*] Prof. M. S. Dresselhaus, Prof. G. Chen, M. Y. Tang, Dr. R. G. Yang, H. Lee  
Massachusetts Institute of Technology  
Cambridge, MA 02139 (USA)  
E-mail: millie@mgt.mit.edu  
Dr. D. Z. Wang, Prof. Z. F. Ren  
Boston College  
Chestnut Hill, MA 02467 (USA)  
Dr. J.-P. Fleurial, Dr. P. Gogna  
Jet Propulsion Laboratory, Caltech  
Pasadena, CA 91109 (USA)

[\*\*] The authors gratefully acknowledge stimulating discussions with Profs. Jean-Paul Issi and Joseph Heremans and support from NASA (NA53-03108) for this work.

try. By that time it was already established that the effectiveness of a thermoelectric material could be linked in an approximate way to the dimensionless thermoelectric figure of merit,  $ZT = S^2\sigma T/\kappa$ , where  $S$ ,  $\sigma$ ,  $T$ , and  $\kappa$  are, respectively, the Seebeck coefficient, electrical conductivity, temperature, and thermal conductivity.<sup>[1]</sup> Over the following 3 decades, 1960–1990, only incremental gains were achieved in increasing  $ZT$ , with the  $(\text{Bi}_{1-x}\text{Sb}_x)_2(\text{Se}_{1-y}\text{Te}_y)_3$  alloy family remaining the best commercial material with  $ZT \approx 1$ . During this 1960–1990 period, the thermoelectrics field received little attention from the worldwide scientific research community. Nevertheless, the thermoelectrics industry grew slowly and steadily, by finding niche applications for space missions, laboratory equipment, and medical applications, where cost and energy efficiency were not as important as energy availability, reliability, predictability, and the quiet operation of equipment.

In the early 1990s, the US Department of Defense (DoD) became interested in the potential of thermoelectrics for new types of applications, and as a result the DoD encouraged the research community to re-examine research opportunities for advancing thermoelectric materials to the point that they could be used more competitively for cooling and power-conversion applications from a performance standpoint. This DoD initiative was successful in stimulating the research community to once again become active in this field and to find new research directions that would lead to thermoelectric materials with better performance. As a result of this stimulation, two different research approaches were taken for developing the next generation of new thermoelectric materials: one using new families of advanced bulk thermoelectric materials,<sup>[2–4]</sup> and the other using low-dimensional materials systems.<sup>[5–8]</sup>

The advanced bulk-materials approach focused on new categories of materials that contained heavy-ion species with large vibrational amplitudes (rattlers) at partially filled structural sites, thereby providing effective phonon-scattering centers. The most prominent of these advanced bulk materials are the so-called phonon-glass/electron-crystal (PGEC) materials<sup>[9]</sup> (such as the partially filled skutterudites based on alloys of  $\text{CoSb}_3$ )<sup>[10]</sup> Regarding the low-dimensional materials approach, two ideas were dominant. Firstly, that the introduction of nanoscale constituents would introduce quantum-con-

finement effects to enhance the power factor  $S^2\sigma$ . Secondly, the many internal interfaces found in nanostructures would be designed so that the thermal conductivity would be reduced more than the electrical conductivity, based on differences in their respective scattering lengths.<sup>[11]</sup>

During the 1990s these two approaches developed independently and mostly in different directions. More recently, the two approaches seem to be coming together again. Firstly, the most successful new bulk thermoelectric materials are host materials containing nanoscale inclusions that are prepared by using chemical approaches.<sup>[12]</sup> Secondly, low-dimensional materials systems are now being assembled as nanocomposites containing a coupled assembly of nanoclusters showing short-range low dimensionality embedded in a host material,<sup>[13,14]</sup> thereby producing a bulk material with nanostructures and many interfaces that scatter phonons more effectively than electrons. In this review article, recent advances in the field of low-dimensional thermoelectrics are summarized with emphasis given to new families of bulk thermoelectric materials that incorporate nanoscale building blocks and show potential for scale-up.

## 2. Proof-of-Principle Studies

There are several concepts behind using low-dimensional materials for enhancing thermoelectric performance. The first phase of the investigation of low-dimensional thermoelectric materials was focused on the development of these concepts and on their experimental proof-of-principle verification. This approach has proved to be of great value to present research directions where composite materials are being specially designed and synthesized for superior thermoelectric performance. The quantities  $S$ ,  $\sigma$ , and  $\kappa$  for conventional 3D crystalline systems are interrelated in such a way that it is very difficult to control these variables independently so that  $ZT$  could be increased. This is because an increase in  $S$  usually results in a decrease in  $\sigma$ , and a decrease in  $\sigma$  produces a decrease in the electronic contribution to  $\kappa$ , following the Wiedemann–Franz law<sup>[15]</sup>. However, if the dimensionality of the material is decreased, the new variable of length scale becomes available for the control of materials properties. Then



*Mildred Dresselhaus is an Institute Professor of Electrical Engineering and Physics at MIT. She has been active in many aspects of materials research and has been involved with low-dimensional thermoelectricity from the very beginning of this research field. She is also heavily involved in the study of nanostructures, especially those based on carbon, and with the broad aspects of energy research. She is the recipient of the National Medal of Science and 21 honorary degrees worldwide. She has served as President of the American Association for the Advancement of Science, Treasurer of the National Academy of Sciences, President of the American Physical Society, and is currently Chair of the Governing Board of the American Institute of Physics. She is also a member of the National Academy of Engineering, the American Philosophical Society, and a Fellow of the American Academy of Arts and Sciences. She served as the Director of the Office of Science at the US Department of Energy in 2000–2001.*

as the system size decreases and approaches nanometer length scales, it is possible to cause dramatic differences in the density of electronic states (see Fig. 1), allowing new opportunities to vary  $S$ ,  $\sigma$ , and  $\kappa$  quasi-independently when the length scale is small enough to give rise to quantum-confinement effects as the number of atoms in any direction ( $x$ ,  $y$ , or  $z$ ) becomes small (e.g., less than ca.  $10^2$ ). In addition, as the dimensionality is decreased from 3D crystalline solids to 2D (quantum wells) to 1D (quantum wires) and finally to 0D (quantum dots), new physical phenomena are also introduced and these phenomena may also create new opportunities to vary  $S$ ,  $\sigma$ , and  $\kappa$  independently. These phenomena are discussed below. Furthermore, the introduction of many interfaces, which scatter phonons more effectively than electrons, or serve to filter out the low-energy electrons at the interfacial energy barriers, allows the development of nanostructured materials with enhanced  $ZT$ , suitable for thermoelectric applications.

The field of low-dimensional thermoelectricity started with the introduction of two strategies: the use of quantum-confinement phenomena to enhance  $S$  and to control  $S$  and  $\sigma$  somewhat independently, and the use of numerous interfaces to scatter phonons more effectively than electrons and to scatter preferentially those phonons that contribute most strongly to the thermal conductivity. Early work was focused on establishing the validity of these concepts/strategies, which were first tested in model periodic 2D quantum-well systems<sup>[6]</sup> and later in 1D quantum wire systems<sup>[5,16]</sup> both from a theoretical standpoint and by experimental demonstration of the proof-of-principle of these concepts.<sup>[6,17]</sup> Three additional concepts, including carrier-pocket engineering,<sup>[8,17,18]</sup> energy filtering,<sup>[19,20]</sup> and the semimetal–semiconductor transition<sup>[21]</sup> have further advanced the potential for using low-dimensional materials to enhance thermoelectric performance. The first demonstration of proof-of-principle that a low-dimensional materials system could enhance thermoelectric performance was for a 2D superlattice consisting of PbTe quantum wells and  $\text{Pb}_{1-x}\text{Eu}_x\text{Te}$  barriers.<sup>[6]</sup> Here it was demonstrated first for n-type PbTe<sup>[6]</sup> and soon thereafter for p-type PbTe<sup>[22]</sup> that  $S^2n$  (where  $n$  is the carrier density) within a quantum well with a width below 4 nm could be increased relative to bulk PbTe. Good agreement was obtained between experiment and theoretical predictions on the dependence of  $S^2n$  on the quantum-well thickness. The reason for emphasizing  $S^2n$  rather than  $S^2$ ,

is that  $n$  and  $\sigma$  are related by  $\sigma = ne\mu$ , where  $e$  is the charge on the electron, and the carrier mobility  $\mu$  is highly sensitive to extrinsic factors such as defects, whereas  $S^2n$  is more closely related to intrinsic materials parameters. Not only were PbTe semiconductor superlattices effective for enhancing  $S^2n$ , but the enhancement was also demonstrated in Si quantum wells in the Si/SiGe system<sup>[17]</sup> where good agreement between experiment and theory was also achieved. Experiments on cross-plane transport in  $\text{Bi}_2\text{Te}_3/\text{Sb}_2\text{Te}_3$  superlattices demonstrated that the scattering of phonons by the interfaces reduced the thermal conductivity more than the electrical conductivity,<sup>[23,24]</sup> thereby establishing proof-of-principle of this second concept, which has since been shown in practice to yield a greater enhancement to  $ZT$  than does the enhancement produced by an increase in  $S^2n$ . Following the experimental demonstration of enhanced thermoelectric performance in 2D superlattices, research moved forward in two different directions. In one direction, advances in superlattice design and growth were pursued, which we summarize next, while in the second research direction ordered structures of lower dimensionality (1D quantum wires and 0D quantum dots) were investigated, as described subsequently.

Because of the lattice mismatch between PbTe and PbSe, efforts to grow a heterostructure of a very thin layer of PbSe between two layers of PbTe, resulted in an ordered array of PbSe quantum-dot structures sandwiched between PbTe layers, following the Volmer–Weber island growth process.<sup>[25,26]</sup> Here the quantum dots are in regular arrays of polygonal structures, of constant size, orientation, and spacing. Harman et al.<sup>[27–29]</sup> were able to grow superlattices of such sandwich structures over thousands of periods to produce a quantum-dot superlattice (QDSL) of composition  $\text{PbTe}/\text{PbSe}_{0.98}\text{Te}_{0.02}$  on top of a  $\text{BaF}_2$  substrate followed by a relatively thin PbTe buffer layer. Using Bi as an n-type dopant for this QDSL, values of  $ZT \sim 1.6$  and 3.5 were achieved at 300 K and ca. 570 K, respectively, as shown in Figure 2.<sup>[27]</sup> Encouraging results were also reported for a p-type QDSL based on using Na as the dopant. The very large  $ZT$  values obtained by using this approach show that in QDSLs it is possible to both increase the power factor  $S^2\sigma$  and to decrease the thermal conductivity at the same time, with the reduction in  $\kappa$  being most important for enhancing  $ZT$ . This model system<sup>[27]</sup> establishes a baseline to which other work can be subsequently compared from a performance standpoint, as scale-up and

lower-cost processes are developed for the practical commercialization of advanced thermoelectric technologies. Thin-film thermoelectric cooling devices based on this model system may someday be utilized for these high-performance characteristics.

Now following the second research direction of going to lower dimensions, the study of quantum wires for thermoelectric applications was pursued.<sup>[30]</sup> One material with very high potential

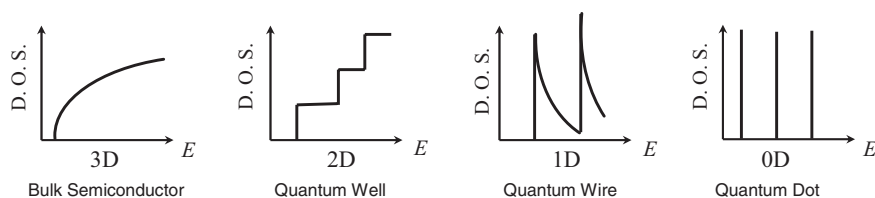


**Figure 1.** Electronic density of states for a) a bulk 3D crystalline semiconductor, b) a 2D quantum well, c) a 1D nanowire or nanotube, and d) a 0D quantum dot. Materials systems with low dimensionality also exhibit physical phenomena, other than a high density of electronic states (DOS), that may be useful for enhancing thermoelectric performance (see text).

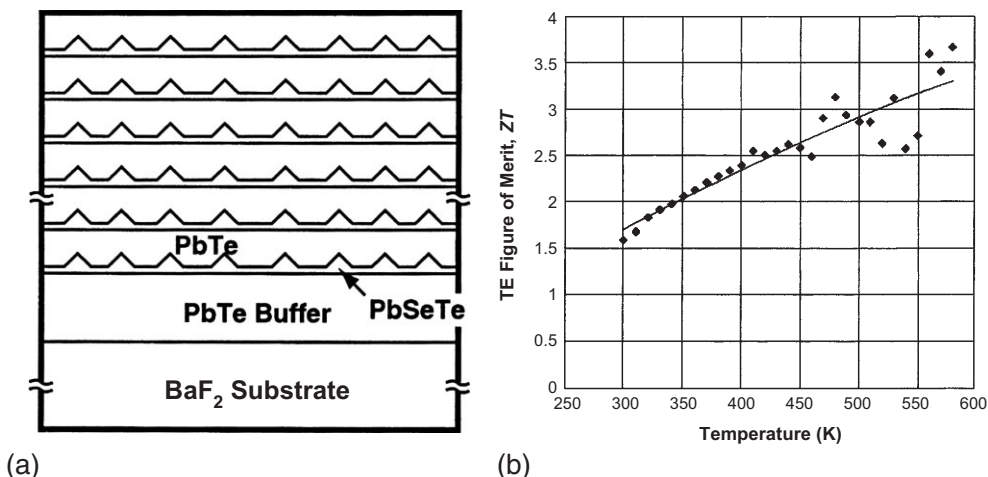


**Figure 2.** a) Schematic drawing of a QDSL [28,29] and b) TE figure of merit vs. temperature for an n-type  $\text{PbSe}_{0.98}\text{Te}_{0.02}/\text{PbTe}$  QDSL sample [27]. Copyright 2005, Minerals, Metals and Materials Society.

for thermoelectric applications has for many years been Bi and Bi-related materials, because of the high  $S$  of the Bi L-point<sup>[31]</sup> electron carriers. But unfortunately, Bi is a semimetal with both electron and hole carriers, and electrons and holes therefore contribute with opposite signs to its total  $S$ . To take advantage of the excellent electronic properties of the electron carriers in Bi materials, they would have to be prepared as an n-type semiconductor. This is possible with the use of either low-dimensional Bi structures or by alloying with Sb, as discussed below. The development of Bi-based quantum-well superlattices was, however, impeded by the difficulty in finding a suitable barrier material for Bi quantum wells in preparing 2D quantum-well superlattices. Therefore, the development of Bi and  $\text{Bi}_{1-x}\text{Sb}_x$  alloys as low-dimensional materials took the form of preparing ordered arrays of 1D quantum wires inside the pores of anodic Al templates: Al is a well-behaved barrier material.<sup>[32]</sup>

The mechanism by which Bi can be converted into a semiconductor is the size-dependent semimetal–semiconductor transition.<sup>[32–34]</sup> When the size of a semimetal nanowire decreases so that there are relatively few quantum states for the direction normal to the axis of the nanowire, then the energy bands split into discrete sub-bands. In this quantum regime, as the wire diameter decreases, the lowest conduction sub-band edge moves up in energy while the highest valence sub-band edge moves down in energy until these energy levels cross as the material makes a transition from a semimetal (with overlapping energy states for the lowest conduction band and the highest valence band) to a semiconductor with a bandgap between the valence and conduction bands (see Fig. 3). In the semiconducting phase, the material can be doped to have one strongly dominant carrier type. Such a semimetal–semiconductor transition was predicted,<sup>[21]</sup> and subsequently observed experimentally.<sup>[7,36]</sup> As alloying Bi with Sb changes the electronic structure of the bulk alloy,<sup>[37]</sup> calculations can be used

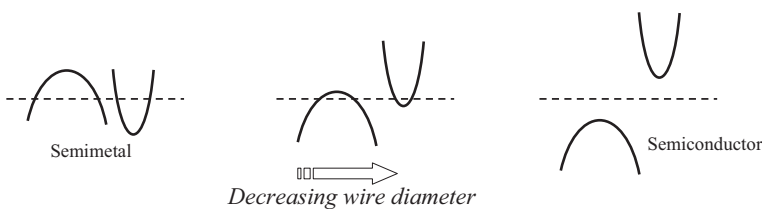


**Figure 3.** Schematic diagram of the Bi nanowire semimetal–semiconductor electronic transition as the lowest conduction sub-band at the L-point and the highest valence sub-band at the T point [35] (Copyright 1968, American Physical Society) moves down in energy, as the nanowire diameter  $d_w$  decreases. a)  $d_w \gg 50$  nm, b)  $d_w = 50$  nm, c)  $d_w \ll 50$  nm, the values being appropriate to pure Bi [5]. Copyright 2003, Massachusetts Institute of Technology.

to show the dependence of the semimetal–semiconductor transition for a Bi–Sb nanowire, on both wire diameter and Sb concentration.<sup>[38,39]</sup> These phenomena have also been confirmed experimentally<sup>[5]</sup> by changing both the wire diameter and Sb composition, thereby providing two variables for controlling and optimizing nanomaterials for enhanced thermoelectric performance.

Superlattices of quantum dots along nanowires have been synthesized experimentally<sup>[40–43]</sup> and calculations have been carried out<sup>[44]</sup> indicating the parameters that should be controlled for enhancing the performance of this type of quantum-dot superlattice along nanowires for thermoelectric applications. However, no proof of principle has yet been demonstrated experimentally for this approach.

Another previously known materials-related concept that has been introduced to enhance the thermoelectric power factor  $S^2\sigma$  is the concept of energy filtering<sup>[19,45,46]</sup> of carriers by the introduction of appropriate barriers in the form of interfaces that restrict the energy of carriers entering a material. At an interface, those carriers with a mean energy substantially above the Fermi level  $E_F$  will pass through the interface preferentially, thereby enhancing the thermopower, which depends of the excess energy ( $E - E_F$ ) of carriers in the sam-

ple.<sup>[19,46]</sup> Using the energy-filtering approach, barriers have been introduced in such a way that the reduction in the electrical conductivity  $\sigma$  is more than compensated for by the increase in  $S$  through the energy-filtering process, thereby resulting in an increase in power factor  $S^2\sigma$ .<sup>[19,45]</sup> All of these concepts and strategies are currently being exploited in improving the performance of nanostructured materials for thermoelectric applications. Both fundamental and applications-oriented studies are now currently being pursued to advance the field.

The concept of carrier-pocket engineering<sup>[47]</sup> has been introduced to design a superlattice structure so that one type of carrier is quantum confined in the quantum-well region and another type of carrier of the same sign is quantum confined in the barrier region. This concept of carrier-pocket engineering was introduced for the case of  $\Gamma$ -point electrons<sup>[31]</sup> for GaAs quantum wells and X-point electrons<sup>[31]</sup> in the AlAs barriers in GaAs/AlAs quantum-well superlattices.<sup>[47]</sup> This concept has also been applied to Si/SiGe 2D superlattices,<sup>[48]</sup> and in some sense is widely used in self-assembled nanostructured composites where all components could be expected to contribute to the enhancement of  $ZT$ .

Up until now, the main gains in increasing  $ZT$  for low-dimensional systems are based on strategies to reduce the thermal conductivity,<sup>[49]</sup> whether by increasing the effect of rattlers in the cages of skutteruditelike materials,<sup>[2]</sup> or by increasing the number of interfaces that scatter phonons more effectively than electrons.<sup>[49]</sup> But to increase  $ZT$  sufficiently to lead to commercialization of low-dimensional thermoelectric materials, it may not be enough to only decrease the thermal conductivity, but it may also be necessary to increase the power factor  $S^2\sigma$  at the same time. It has already been demonstrated that this approach is possible in QDSL systems and in nanocomposite thermoelectric materials as described below.

### 3. Nanocomposite Thermoelectric Materials

As thermal conductivity reduction is a major mechanism behind the enhanced figure of merit in superlattices, and past studies on the heat-conduction mechanisms in superlattices conclude that periodic structures are not necessary for thermal-conductivity reduction, nanocomposites then become a natural step for extending the success in superlattices to more scalable materials.<sup>[50]</sup>

At the present time a number of research groups are developing nanocomposite materials with a potential for scale-up and practical applications. The goals for designing materials for such applications are to introduce many interfaces that are specially chosen to: 1) reduce the thermal conductivity more than the electrical conductivity by interface scattering, and 2) to increase  $S$  (for example, by carrier-energy filtering or by quantum confinement) more than decreasing the electrical conductivity, thereby yielding an increase in power factor, with both goals helping to increase  $ZT$ . Nanocomposite thermoelectric materials offer a promising approach for the prep-

aration of bulk samples with nanostructured constituents. Such nanocomposite materials are easily handled from a properties-measurement/materials-characterization point of view; they can be assembled into a variety of desired shapes for device applications, and they can be scaled up for commercial applications. In this report we show preliminary results to verify that: 1) a random assemblage of two kinds of nanoparticles in a heterogeneous composite or of nanoparticles in a host material (see Fig. 4 for this conceptualization of a nanocomposite) of bulk length scale (several millimeters in size)

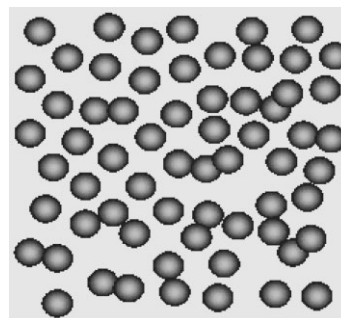


**Figure 4.** Conceptualization of a nanocomposite material with nanoparticles embedded in a host material, as for example Si nanoparticles (melting point 1687 K) in a Ge host material (melting point 1211 K) [13]. Copyright 2005, Materials Research Society. Similarly, nanocomposite materials of rather similar properties can be prepared from hot-pressing two different nanoparticle constituents, such as Si and Ge nanoparticles.

can yield enhanced thermoelectric performance relative to the alloy with the same composition of constituents, 2) a thermal conductivity reduction can be realized over a wide temperature range, 3) the power factor can be increased at the same time by increasing  $S$  more than  $\sigma$  is decreased and, 4) that the nanostructures of the constituent materials can be preserved during the processing steps used to prepare the nanocomposite material. Conceptual advances are here presented for designing effective nanocomposite materials with enhanced thermoelectric performance along with explicit experimental results shown for Si–Ge nanocomposite materials. A variety of materials synthesis processes and approaches have been suggested by various research groups,<sup>[51–53]</sup> involving different materials systems and processing methods, utilizing a number of common fundamental concepts, but differing in detail in their execution. We also report here briefly on some of these advances.

Model calculations provide an important guide for the design and choice of processing parameters in the preparation of nanocomposite structures. As the reduction of the thermal conductivity  $\kappa$  is the most important strategy for enhancing the thermoelectric figure of merit for nanocomposites,<sup>[49]</sup> calculations to demonstrate how nanocomposites might be designed to have a  $\kappa$  value lower than that for alloys of the same nominal composition of constituents are of great interest. Such calculations suggest the choice of processing parameters and approaches to be taken for doping and other process-sen-

sitive considerations in the actual preparation of nanocomposite materials. Two approaches for carrying out such model calculations have been: 1) Solution of the Boltzmann transport equation for a unit cell containing aligned nanoparticles with periodic boundary conditions imposed on the heat-flow direction, with a fixed temperature difference across each unit cell in the model nanocomposite, and with the interface reflectivity and the relaxation time used as input parameters.<sup>[50]</sup> 2) A Monte Carlo method has also been used for the modeling calculations, particularly for the case of random particle size, orientation, and distribution.<sup>[54]</sup> Checks between the two calculational approaches have been carried out successfully, and the types of particle distributions that have been considered in the model calculations are shown in Figure 5.<sup>[55,56]</sup>



Figure 5. Types of particle distributions that have been used in model calculations [54,55]. Copyright 2005, Massachusetts Institute of Technology.

The model calculations show that the thermal conductivity for nanocomposites can fall below that obtained for their parent bulk samples for cases where the composites contain particle sizes in the 10 nm range for  $\text{Si}_x\text{Ge}_{1-x}$  alloy compositions in the range of  $0.2 < x < 0.8$ . It is interesting to point out in Figure 6 the fundamental differences between bulk alloy samples and nanostructured samples of the same composition. In this figure the thermal conductivity along the wire direction is plotted versus the volumetric fraction of Si for nanostructures

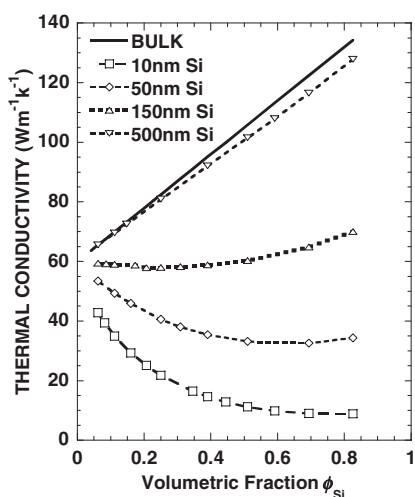


Figure 6. Calculated thermal conductivity vs. increasing Si fraction for Si nanowires in a Ge host material to constitute a model for the thermal conductivity of  $\text{Si}_x\text{Ge}_{1-x}$  nanocomposite samples. For comparison, results are shown (solid line) for a bulk alloy with the same chemical composition as the nanocomposite material [55,56]. Copyright 2005, American Physical Society. Transport here is along the wire direction.

of different cross-sectional widths  $d_w$  in comparison to the bulk alloy of the same composition. For bulk alloys or nanostructured composites based on nanostructures of large  $d_w$  size (ca. 500 nm), Figure 6 shows that the lattice thermal conductivity increases with increasing Si concentration, reflecting the higher bulk thermal conductivity and higher sound velocity of Si relative to Ge.<sup>[56]</sup> However, for nanostructural widths of 50 nm or less, the mean free path is limited by the nanostructural width  $d_w$ , so that the thermal conductivity  $\kappa$  now becomes more sensitive to the velocity of sound and specific heat rather than to the bulk mean free path for scattering. In this regime,  $\kappa$  decreases with increasing volumetric fraction of Si (see Fig. 6), in contrast to the behavior of the 3D alloy samples with similar chemical composition, because the effective thermal conductivity of Si drops more from the interference scattering than from other mechanisms. The calculations plotted in Figure 7 further show that Si-Ge nanocomposites with 10 nm or 50 nm Si wires can have lower thermal conduc-

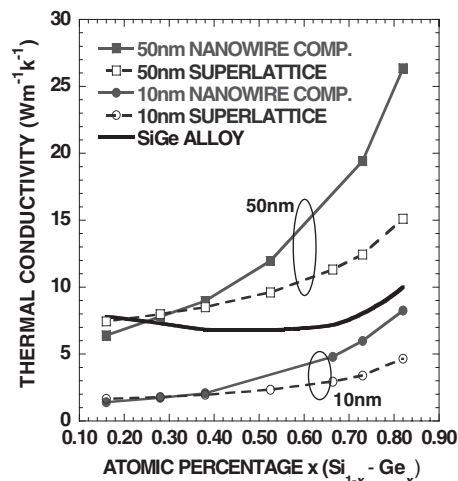
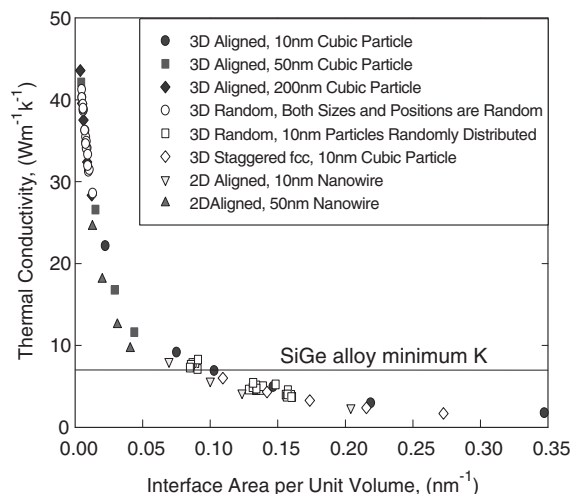


Figure 7. Calculated thermal conductivity of a SiGe composite material containing Si nanowires in a Ge host material. Transport is here normal to the wire direction [55,57]. Copyright 2004, American Physical Society.

tivity than that of Si-Ge superlattices (multilayers) with the same dimension of Si film thickness at the same  $\text{Si}_x\text{Ge}_{1-x}$  stoichiometry (when  $x > 0.60$ ). These results show the possibility of fabricating cost-effective nanocomposites with a thermal conductivity lower than that of expensive superlattices. Monte Carlo simulations were carried out for many different mean particle sizes, size distributions, and degrees of randomness, and the results show that the thermal conductivity depends sensitively on the interface density (interface area per unit volume), following a universal curve as shown in Figure 8. Provided that the interface area per unit volume is above  $0.08 \text{ nm}^{-1}$ , the thermal conductivity of the nanocomposite is lower than that of the bulk alloy for these kinds of samples. These results strongly indicate that ordered structures are not necessary to achieve a low thermal conductivity, thus validating the use of self-assembled nanocomposite materials, such



**Figure 8.** Universal curve for the thermal conductivity of Si nanoparticles and nanowires in a SiGe host material showing that nanoparticle and nanowire composites can give rise to very low thermal conductivity values, much lower than the minimum thermal conductivity value of a SiGe alloy [54,55]. Copyright 2005, Massachusetts Institute of Technology. The value of the minimum thermal conductivity is taken from the work of Abeles [58]. Copyright 1963, American Physical Society.

as in Figures 4 and 5 for enhancing thermoelectric performance. In fact, it was early modeling and measurement work, showing that it is not necessary to have coherent interface structures to reduce the thermal conductivity, that led to the proposal of self-assembled nanocomposites (Fig. 4) for thermoelectric applications in the first place.<sup>[24]</sup>

To synthesize nanostructured composite materials, nanoparticles of the constituent materials Si, Ge, and  $\text{Si}_x\text{Ge}_{1-x}$  alloys were prepared using either wet-chemistry, ball-milling, or by inert-gas condensation methods.<sup>[13]</sup> Nanoparticles of both Si and Ge were prepared using either nanometer- or micrometer-sized particles. These particles were then either hot-pressed (HP) using a plasma pressure compaction ( $\text{P}^2\text{C}$ ) method or HP in argon at 1333 K, yielding dense, mechanically strong, bulk nanocomposites of near theoretical density. Disks a half inch in diameter (1 inch  $\approx$  2.54 cm) and samples of other shapes were thus prepared. Many different conditions of compaction and levels of n- and p-type doping were used to study the dependence of the nanocomposite materials on the processing conditions and materials parameters. Different sample shapes were used for different materials characterization measurements. Some optimization of the processing conditions was carried out for maximizing the figure of merit along with providing improved in-service properties. Each set of samples, grown with deliberately chosen processing parameters, was then characterized by using X-ray, scanning electron microscopy (SEM), and transmission electron microscopy (TEM) techniques to verify and characterize the nanoparticle integrity, meaning that nanoparticle inclusions remained in the nanocomposite after all the processing steps were completed. The X-ray and TEM characterization results show that small nanoparticles of 5–10 nm size were retained

after our nanoparticle  $\text{P}^2\text{C}$  procedures were carried out in the 1050–1100 °C range. Materials science studies of the effect of porosity on the transport properties show that the electrical conductivity of the nanocomposite changes by orders of magnitude when the sample density changes by only a few percent. Our measurements highlight what we think is a general result, that it is of great importance to achieve close to theoretical materials density for thermoelectric nanocomposite materials, especially for the compaction of nanometer-sized particles relative to the compaction of micrometer-sized particles.

A comparison between preliminary experimental results for two samples and modeling calculations based on  $\text{Si}_x\text{Ge}_{1-x}$  nanocomposite materials is shown in Figure 9. The results show a low value for the experimental thermal conductivity

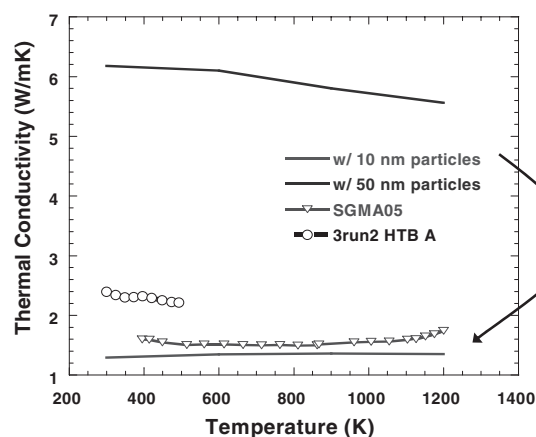


**Figure 9.** Comparison between experimental measurements on two nanocomposite samples and model calculations for the temperature dependence of the thermal conductivity for nanocomposites containing 10 and 50 nm Si nanoparticles in a Ge host. The mean particle sizes for the experimental samples are indicated (see text) [13]. Copyright 2005, Materials Research Society.

over a wide temperature range for a p-type  $\text{Si}_{0.80}\text{Ge}_{0.20}\text{B}_{0.016}$  sample containing nanoparticles that had been ball-milled for 96 h. The calculated curve shown for comparison is based on the modeling results for 10 nm Si nanoparticles embedded in a Ge host material. Preliminary results on a sample prepared by using the  $\text{P}^2\text{C}$  method, and measured only up to 500 K, show a higher thermal conductivity than that for the ball-milled sample, but nevertheless with an interesting reduction in thermal conductivity through the sample-processing and preparation steps.

Experimental transport results given in Figure 10 for an experimental sample (SGMA04), similar to the one used in Figure 9 (SGMA05), show that, due to strong interface scattering, nanocomposite materials can have a higher resistivity and a higher  $S$  than bulk thermoelectric materials. As the increase in  $S$  for the nanostructured material prepared at the Jet Propulsion Laboratory (JPL) by ball-milling (likely because of energy-filtering effects) is substantially larger than the de-

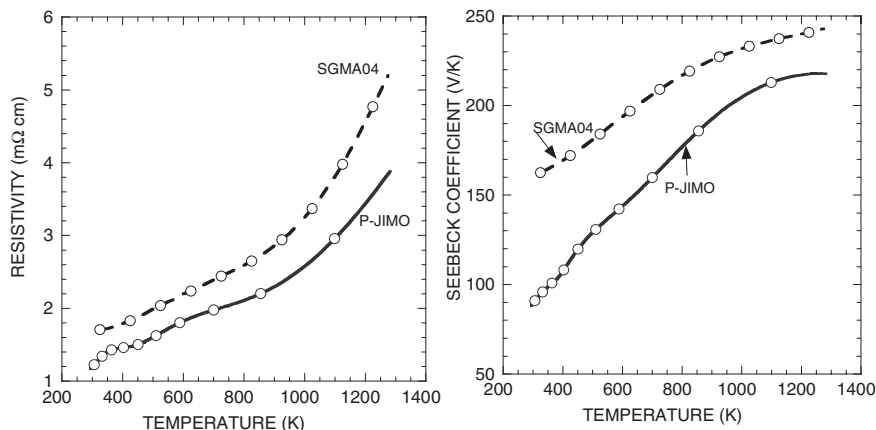


**Figure 10.** Comparison between the temperature-dependent resistivity and  $S$  of a p-type sample of a  $\text{Si}_{0.80}\text{Ge}_{0.20}\text{B}_{0.016}$  nanocomposite material, of the indicated nominal composition, obtained by ball-milling the starting material for 96 h (SGMA04) in comparison to a bulk/advanced SiGe alloy material (P-JIMO) developed for thermoelectric applications, showing that the power factor can be increased and the thermal conductivity can be reduced at the same time in these nanocomposite material samples [13,59]. Copyright 2005, Materials Research Society.

crease in  $\sigma$ , the power factor is shown to increase in actual experimental nanocomposites samples over most of the temperature range (see Fig. 11), consistent with predictions from model calculations.<sup>[55,59]</sup> Also shown in Figure 11 is a comparison between the thermal conductivity for a nanocomposite and an advanced bulk thermoelectric material, showing that it is possible for a nanocomposite material to increase its power factor and to decrease its thermal conductivity at the same time. Such behavior only occurs for nanostructured systems.

Figure 12 shows the temperature dependence of  $ZT$  (between 300 and 1300 K) for several SiGe samples, showing that the best thermoelectric performance is achieved in the  $\text{Si}_{0.80}\text{Ge}_{0.20}\text{B}_{0.016}$  sample doped with 1.6% boron and ball-milled for 96 h and that the sample with 2.0% boron doping,

and similar otherwise, showed the second best thermoelectric performance. Although the measurements on the nanocomposites prepared by using the P<sup>2</sup>C method have only been measured up to about 500 K, they also seem promising. As the nanocomposite thermoelectric materials are still at an early stage of development, especially related to optimizing their processing conditions and doping levels and doping species, further improvements in  $ZT$  are expected for self-assembled nanocomposite materials based on the concept presented in Figure 11 showing that it is possible to increase  $S^2\sigma$  and to reduce  $\kappa$  at the same time.

Experimental measurements and detailed theoretical analysis of two model systems (PbTe with metal nanoparticle inclusions and  $\text{In}_{0.53}\text{Ga}_{0.47}\text{As}$  with ErAs nanoparticles) shed much light on a strategy for embedding nanoparticles into a host material to enhance its thermoelectric performance. In the case of the PbTe system, metallic nanoparticles are embedded in a PbTe host material and the mechanism responsible for the increase in  $S$  was studied in some detail.<sup>[60,61]</sup> For the  $\text{In}_{0.53}\text{Ga}_{0.47}\text{As}$  system, nanometer-sized semimetallic ErAs particles were embedded in the host material and the mechanism responsible for the measured reduction in the thermal conductivity was determined.<sup>[62]</sup> In both cases insights into scattering mechanisms associated with nanosystems were shown to be beneficial to thermoelectric performance, as described below in more detail. New insights about novel scattering mechanisms associated with metallic nanoparticles (Pb or Ag) embedded in a PbTe host material were obtained from detailed

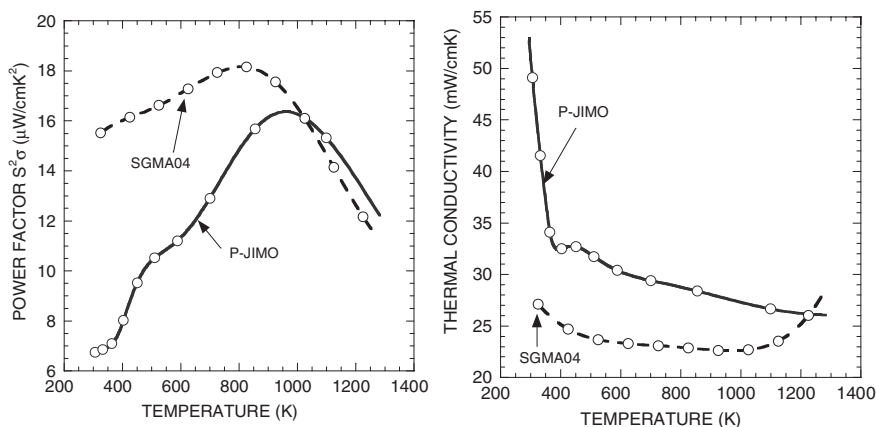


**Figure 11.** Comparison between the temperature-dependent power factor and the thermal conductivity for a p-type  $\text{Si}_{0.80}\text{Ge}_{0.20}\text{B}_{0.016}$  nanocomposite material produced by ball-milling the starting materials for 96 h and a bulk SiGe alloy material developed for thermoelectric applications, showing that the power factor can be increased and the thermal conductivity reduced at the same time in the nanocomposite material [13,59]. Copyright 2005, Materials Research Society.

temperature-dependent measurements of four transport properties: the electrical conductivity  $\sigma$ , the Seebeck Coefficient  $S$ , the Hall coefficient  $R_H$ , and the isothermal transverse Nernst–Ettingshausen coefficient  $N$ .<sup>[60]</sup> This allows a determination to be made of four materials parameters important to thermoelectric performance as a function of temperature, namely the carrier density ( $n$  or  $p$ ), the carrier mobility  $\mu$ , the effective mass  $m_d^*$ , and the scattering parameter  $\lambda$ , which is defined by the energy dependence of the carrier-scattering-relaxation parameter  $\tau = \tau_0 E^{\lambda-1/2}$  where  $\tau_0$  is an energy-independent scaling coefficient. In these experiments it is the isothermal transverse Nernst–Ettingshausen coefficient  $N$  that is most sensitive to  $\lambda$ , and it is the scattering pa-

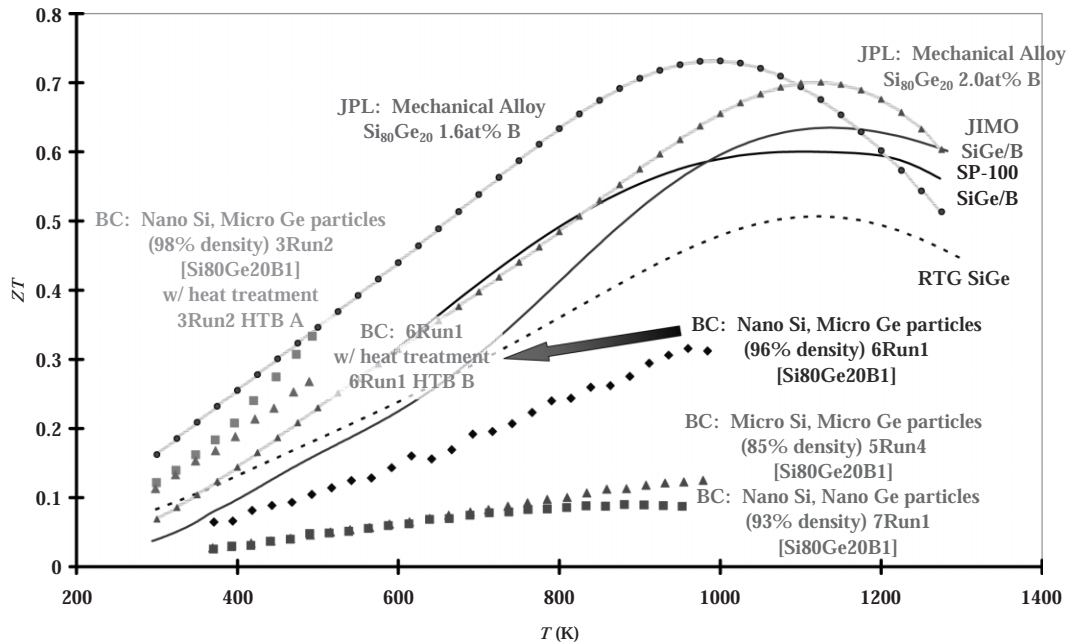


**Figure 12.** Plot of  $ZT$  versus temperature for a  $\text{Si}_{0.80}\text{Ge}_{0.20}\text{B}_{0.016}$  sample prepared by ball-milling (mechanical alloy) as compared to the radioisotope thermoelectric generators (RTGs)  $\text{SiGe}$  bulk materials now used in NASA (National Aeronautics and Space Administration) flights and to both a variety of JIMO (Jupiter Icy Moons Orbiter) test samples (labeled JIMO) and a few of the nanocomposites obtained by hot-pressing (using the  $\text{P}^2\text{C}$  method) nanoparticles prepared by using the wet-chemistry method [13]. Copyright 2005, Materials Research Society.

parameter  $\lambda$  that is most sensitively modified by the inclusion of nanoscale metallic particles in the  $\text{PbTe}$  host material. For bulk  $\text{PbTe}$ ,  $\lambda$  is found to be in the range  $0.2 < \lambda < 0.7$ , whereas for the metallic nanoparticles  $\lambda$  is found to be greater than 3. No known scattering mechanism has such a large  $\lambda$  value. The larger the value of  $\lambda$ , the larger the energy-filtering effect, and the larger the enhancement of the Seebeck effect. Analysis of the published results on the carrier-concentration dependence of  $S$  of the quantum-dot superlattices of  $\text{PbTe}$  with  $\text{PbSe}$  nanoparticle inclusions<sup>[28]</sup> shows consistent behavior to that of the  $\text{Pb}$  and  $\text{Ag}$  metallic inclusions.<sup>[60]</sup> Similar behavior was also reported for a nanocomposite composed of sintered powders of nanometer-sized grains.<sup>[61]</sup> When taken together, it is concluded that nanoparticles exhibit an energy-filtering effect,<sup>[63]</sup> which strongly lengthens the relaxation time of the high-energy electrons relative to their behavior in the corresponding bulk material. These studies teach us that nanoparticle inclusions through a size-dependent energy-filtering effect can enhance  $S$  significantly. The studies on the  $\text{Si}_x\text{Ge}_{1-x}$  nanocomposite yield results consistent with these findings, showing further that the increase in  $S$  is sufficiently larger than the decrease in the electrical conductivity so that the power factor is increased.<sup>[59]</sup>

Study of the mechanism responsible for the large reduction in the thermal conductivity of  $\text{In}_{0.53}\text{Ga}_{0.47}\text{As}$  containing semimetallic  $\text{ErAs}$  nanoparticles provides a different set of important insights about large changes in the behavior of thermoelectric materials when they contain nanoparticles inclu-

sions.<sup>[62]</sup> Using  $\text{ErAs}$  nanoparticles with a size of about 1–4 nm, two types of samples were prepared by using molecular-beam epitaxy, such that the  $\text{ErAs}$  nanoparticles were arranged in either: 1) a superlattice structure or 2) a random distribution within the bulk material. The analysis of the thermal-conductivity measurements was carried out on the basis of Mathiessen's rule, whereby the effective scattering rate is the sum of the scattering rates due to the various phonon-scattering processes, including boundary scattering, umklapp scattering, defect or alloy scattering, electron–phonon scattering, and  $\text{ErAs}$  nanoparticle scattering. Analysis of the experimental temperature-dependent thermal-conductivity results from 50 to 800 K shows that the phonon scattering by  $\text{ErAs}$  nanoparticles is the dominant additional factor contributing to phonon scattering for both types of samples. The analysis further shows that both types of samples achieve lower thermal conductivities than the minimal thermal conductivity for bulk materials proposed by Slack,<sup>[9]</sup> in agreement with the results presented above on  $\text{Si}_x\text{Ge}_{1-x}$  nanocomposite thermoelectric materials.<sup>[13]</sup>

Theoretical analysis of the phonon scattering by a nanoparticle showed that mid- to long-wavelength phonons were scattered more effectively, whereas atomic-scale defects in the  $\text{In}_{0.53}\text{Ga}_{0.47}\text{As}$  host material scattered the Brillouin-zone-edge phonons more effectively. For this reason the  $\text{ErAs}$  nanoparticles were especially effective in scattering those phonons that contribute strongly to the thermal conductivity. However, the size distribution of the nanoparticles in the samples served to

scatter phonons over a wide range of phonon wavelengths. The effect of the nanoparticles was to increase  $ZT$  by more than a factor of two, with most of the enhancement coming from the thermal-conductivity effect. Thin film samples of the  $\text{In}_{0.53}\text{Ga}_{0.47}\text{As}$  host material in which ErAs nanoparticles are embedded might be useful for the cooling of on-chip electronics.

This work teaches us that nanoparticles also perform an energy-filtering effect that preferentially scatters those phonons that contribute strongly to the thermal conductivity. The work further confirms, what was shown in the studies of  $\text{Si}_x\text{Ge}_{1-x}$  nanocomposites, that ordering of the nanoparticles in the host matrix is not important for reducing the thermal conductivity.

#### 4. Conclusions and Outlook

In summary, these studies on nanocomposite thermoelectrics show that randomly distributed nanostructures in SiGe nanocomposite materials can lead to a reduction in the thermal conductivity below that of an alloy of the same overall chemical stoichiometry. Even though the electrical resistivity may increase as a result of the introduction of nanoparticles, the increase in  $S$  can be significantly larger, so that the power factor can increase as a result of nanostructuring. Furthermore, both an increase in the power factor and a decrease in the thermal conductivity relative to an alloy sample of the same composition can occur in a given sample at the same time, thereby resulting in an increase in  $ZT$  from both processes. These findings identify promising research directions for nanocomposite materials produced either by materials processing strategies as in this work or by chemical means as shown for other materials systems.

This review leaves us with several take-home messages for future research directions for advanced thermoelectric materials based on nanostructures. Proper choice of materials processing conditions is essential for achieving the desired enhancement in  $ZT$  for a given materials system and for making the process suitable for scale-up applications. The processing conditions must first be optimized so that the desired microstructure, mean particle size (nanoscale), particle size distribution, materials densification, and grain-boundary properties will be maintained both through the processing steps and through the service time of the thermoelectric devices as they are used, thus giving a long-term stability to the desired nanostructure at high temperature and under required service conditions. One approach to overcome these challenges is to create a nanocomposite with at least two different phases to prevent grain growth during processing and a second approach involves the use of nanometer-sized dopant particles to provide a more homogeneously doped material for device fabrication. Modeling is expected to play a major role in suggesting strategies for the optimization of processes for materials selection, for selection of the particle-size distribution, and for the design of interfaces to maximize phonon scattering relative to charge-carrier scattering. As every materials system

has different detailed properties and constraints, the study of several materials systems as a basis for preparing high-performance nanostructured composites is recommended. The knowledge gained from one system would give ideas useful for the advance of the preparation of other materials systems.

Received: March 13, 2006

Revised: September 20, 2006

Published online: March 23, 2007

- [1] H. J. Goldsmid, *Thermoelectric Refrigeration*, Plenum Press, New York **1964**.
- [2] D. T. Morelli, T. Caillat, J.-P. Fleurial, A. Borshchevsky, J. Vander-sande, B. Chen, C. Uher, *Phys. Rev. B: Condens. Matter Mater. Phys.* **1995**, *51*, 9622.
- [3] G. S. Nolas, D. T. Morelli, T. M. Tritt, *Annu. Rev. Mater. Sci.* **1999**, *29*, 89.
- [4] T. Caillat, A. Borshchevsky, J.-P. Fleurial, *J. Appl. Phys.* **1996**, *80*, 4442.
- [5] Y.-M. Lin, *Ph.D. Thesis*, Massachusetts Institute of Technology **2003**.
- [6] L. D. Hicks, T. C. Harman, X. Sun, M. S. Dresselhaus, *Phys. Rev. B: Condens. Matter Mater. Phys.* **1996**, *53*, R10493.
- [7] J. Heremans, in *Thermoelectric Materials 2003—Research and Applications*, *MRS Symp. Proc.* (Eds: G. S. Nolas, J. Yang, T. P. Hogan, D. C. Johnson), Materials Research Society Press, Pittsburgh, PA 2004, pp. 3–14.
- [8] T. Koga, S. B. Cronin, M. S. Dresselhaus, in *Thermoelectric Materials—The Next Generation Materials for Small-Scale Refrigeration and Power Generation Applications*, *MRS Symp.* (Eds: T. M. Tritt, G. S. Nolas, G. Mahan, M. G. Kanatzidis, D. Mandrus), Materials Research Society Press, Pittsburgh, PA, 2000, pp. Z4.3.1–4.3.6.
- [9] G. Slack, in *CRC Handbook of Thermoelectrics* (Ed: D. M. Rowe), CRC Press, Boca Raton, FL **1995**.
- [10] C. Uher, in *Thermoelectrics Handbook: Macro to Nano* (Ed: D. M. Rowe), Taylor and Francis, CRC, Boca Raton, FL **2006**, Ch. 34, p. 34.1–34.17.
- [11] a) G. Chen, *Phys. Rev. B: Condens. Matter Mater. Phys.* **1998**, *57*, 14958. b) G. Chen, in *Proc. 1996 Int. Mech. Eng. Congress*, Vol. 59, AMSE, New York, **1996**, pp. 13–23.
- [12] K. F. Hsu, S. Loo, F. Guo, W. Chen, J. S. Dyck, C. Uher, T. Hogan, E. K. Polychroniadis, M. G. Kanatzidis, *Science* **2004**, *303*, 818.
- [13] M. S. Dresselhaus, G. Chen, M. Y. Tang, R. G. Yang, H. Lee, D. Z. Wang, Z. F. Ren, J. P. Fleurial, P. Gogna, in *Materials and Technologies for Direct Thermal-to-Electric Energy Conversion*, *MRS Symp. Proc.* (Eds: J. Yang, T. P. Hogan, R. Funahashi, G. S. Nolas), Materials Research Society Press, Pittsburgh, PA **2005**, pp. 3–12.
- [14] M. S. Dresselhaus, J. P. Heremans, in *Thermoelectrics Handbook: Macro to Nano* (Ed: D. M. Rowe), Taylor and Francis, CRC, Boca Raton, FL **2006**, Ch. 39, p. 39.1–39.24.
- [15] a) A. Bejan, A. D. Allan, *Heat Transfer Handbook* Wiley, New York, **2003**, p. 1338. b) Wiedemann–Franz law [http://en.wikipedia.org/wiki/Wiedemann\\_franz\\_law](http://en.wikipedia.org/wiki/Wiedemann_franz_law) (accessed February 2007).
- [16] Y.-M. Lin, S. B. Cronin, J. Y. Ying, M. S. Dresselhaus, J. P. Heremans, *Appl. Phys. Lett.* **2000**, *76*, 3944.
- [17] T. Koga, S. B. Cronin, M. S. Dresselhaus, J. L. Liu, K. L. Wang, *Appl. Phys. Lett.* **2000**, *77*, 1490.
- [18] T. Koga, *Ph.D. Thesis*, Harvard University **2000**.
- [19] B. Y. Moizhes, V. A. Nemchinsky, in *Proc. for the 11th Int. Conf. on Thermoelectrics*, University of Texas, Arlington, TX **1992**.
- [20] Y. I. Ravich, B. A. Efimova, V. I. Tamarchenko, *Phys. Status Solidi B* **1971**, *48*, 453.
- [21] L. D. Hicks, T. C. Harman, M. S. Dresselhaus, *Appl. Phys. Lett.* **1993**, *63*, 3230.
- [22] T. C. Harman, P. J. Taylor, D. L. Spears, M. P. Walsh, in *Proc. for the 18th Int. Conf. on Thermoelectrics*, AIP, New York **1999**.

- [23] R. Venkatasubramanian, in *Semiconductors and Semimetals: Recent Trends in Thermoelectric Materials Research III* (Ed: T. M. Tritt), Academic, San Diego, CA **2001**, Ch. 4, pp. 175–201.
- [24] B. Yang, G. Chen, in *Chemistry, Physics, and Materials Science for Thermoelectric Materials: Beyond Bismuth Telluride* (Eds: M. G. Kanatzidis, T. P. Hogan, S. D. Mahanti), Kluwer Academic/Plenum Publishers, New York **2003**, pp. 147–167.
- [25] G. Springholz, V. Holy, M. Pinczolits, P. Bauer, G. Bauer, *Science* **1998**, *282*, 734.
- [26] G. Springholz, M. Pinczolits, P. Mayer, V. Holy, G. Bauer, H. Kang, L. Salamanca-Riba, *Phys. Rev. Lett.* **2000**, *84*, 4669.
- [27] T. C. Harman, M. P. Walsh, B. E. LaForge, G. W. Turner, *J. Electron. Mater.* **2005**, *34*, L19.
- [28] T. C. Harman, P. J. Taylor, M. P. Walsh, B. E. LaForge, *Science* **2002**, *297*, 2229.
- [29] T. C. Harman, P. J. Taylor, M. P. Walsh, D. L. Spears, *J. Electron. Mater.* **2000**, *29*, L1.
- [30] M. S. Dresselhaus, Y.-M. Lin, S. B. Cronin, O. Rabin, M. R. Black, G. Dresselhaus, T. Koga, in *Semiconductors and Semimetals: Recent Trends in Thermoelectric Materials Research III* (Ed: T. M. Tritt), Academic, San Diego, CA **2001**, Ch. 1, pp. 1–121.
- [31] a) P. Y. Yu, M. Cardona, *Fundamentals of Semiconductors—Physics and Material Properties*, 3rd Edition, Springer, Berlin **2001**, p. 22.  
b) Britney Spears Guide to Semiconductor Physics, Semiconductor Crystals, Figure 7.  
<http://britneyspears.ac/physics/crystals/wcrystals.htm> (accessed February 2007).  
c) Mathematical Methods in Nanophotonics, lecture notes, Figure 93.  
<http://math.mit.edu/~stevenj/18.325/fccbz.pdf> (accessed February 2007).
- [32] Y.-M. Lin, M. S. Dresselhaus, J. Y. Ying, in *Advances in Chemical Engineering* (Ed: K. Ricci), Academic, York, PA **2001**, Ch. 5, pp. 167–203.
- [33] S. Takaoka, K. Murase, *J. Phys. Soc. Jpn.* **1985**, *54*, 2250.
- [34] J. Heremans, C. M. Thrush, Y.-M. Lin, S. Cronin, Z. Zhang, M. S. Dresselhaus, J. F. Mansfield, *Phys. Rev. B: Condens. Matter Mater. Phys.* **2000**, *61*, 2921.
- [35] See Figure 1 of this paper: S. H. Koenig, A. A. Lopez, *Phys. Rev. Lett.* **1968**, *20*, 48.
- [36] J. Heremans, C. M. Thrush, D. T. Morelli, M.-C. Wu, *Phys. Rev. Lett.* **2003**, *91*, 076 804.
- [37] A. L. Jain, *Phys. Rev.* **1959**, *114*, 1518.
- [38] O. Rabin, *Ph. D. Thesis*, Massachusetts Institute of Technology **2004**.
- [39] O. Rabin, Y.-M. Lin, M. S. Dresselhaus, *Appl. Phys. Lett.* **2001**, *79*, 81.
- [40] L. Piraux, J. M. George, J. F. Despres, C. Leroy, *Appl. Phys. Lett.* **1994**, *65*, 2484.
- [41] Y. Wu, R. Fan, P. Yang, *Nano Lett.* **2002**, *2*, 83.
- [42] M. S. Gudiksen, L. J. Lauhon, J. Wang, D. Smith, C. M. Lieber, *Nature* **2002**, *415*, 617.
- [43] M. T. Björk, B. J. Ohlsson, T. Sass, A. I. Persson, C. Thelander, M. H. Magnusson, K. Deppert, L. R. Wallenberg, L. Samuelson, *Nano Lett.* **2002**, *2*, 83.
- [44] Y.-M. Lin, M. S. Dresselhaus, *Phys. Rev. B: Condens. Matter Mater. Phys.* **2003**, *68*, 075 304.
- [45] T. E. Humphrey, M. F. O'Dwyer, H. Linke, *J. Phys. D: Appl. Phys.* **2004**, *38*, 2051.
- [46] Y. I. Ravich, in *CRC Handbook of Thermoelectrics* (Ed: D. M. Rowe), CRC Press, New York **1995**, pp. 67–73.
- [47] T. Koga, X. Sun, S. B. Cronin, M. S. Dresselhaus, *Appl. Phys. Lett.* **1998**, *73*, 2950.
- [48] T. Koga, X. Sun, S. B. Cronin, M. S. Dresselhaus, *Appl. Phys. Lett.* **1999**, *75*, 2438.
- [49] G. Chen, M. S. Dresselhaus, G. Dresselhaus, J.-P. Fleurial, T. Caillat, in *International Materials Review*, Vol. 48 (Ed: M. J. Bevis), Institute of Materials Journals, London **2003**, pp. 45–66.
- [50] R. G. Yang, G. Chen, *Phys. Rev. B: Condens. Matter Mater. Phys.* **2004**, *69*, 195 316.
- [51] T. M. Tritt, J. He, B. Zhang, N. Gothard, D. Thompson, E. Weeks, T. Xiaofeng, K. Aaron, X. Ji, J. W. Kolis, in *Thermoelectric Materials 2005—Research and Applications*, MRS Symp. Proc. (Eds: G. S. Nolas, J. Yang, T. P. Hogan, D. C. Johnson), Materials Research Society, Pittsburgh, PA **2005**, p. F2.1.
- [52] J. P. Heremans, in *Materials and Technologies for Direct Thermal-to-Electric Energy Conversion MRS Proceedings* (Eds: J. Yang, T. P. Hogan, R. Funahashi, G. S. Nolas), Vol. 886, Materials Research Society, Pittsburgh, PA **2005**, pp. 0886-F04-10.1–0886-F04-10.12.
- [53] A. Shakouri, in *Thermoelectric Materials 2005—Research and Applications*, MRS Symp. Proc. (Eds: G. S. Nolas, J. Yang, T. P. Hogan, D. C. Johnson), Materials Research Society Press, Pittsburgh, PA **2005**, p. F7.1.
- [54] M.-S. Jeng, R. Yang, G. Chen, *J. Heat Transfer*, in press.
- [55] R. Yang, *Ph.D. Thesis*, Massachusetts Institute of Technology **2005**.
- [56] R. Yang, G. Chen, M. S. Dresselhaus, *Phys. Rev. B: Condens. Matter Mater. Phys.* **2005**, *72*, 125 418.
- [57] R. Yang, G. Chen, *Phys. Rev. B: Condens. Matter Mater. Phys.* **2004**, *69*, 195 316.
- [58] B. Abeles, *Phys. Rev.* **1963**, *131*, 1906.
- [59] R. Yang, G. Chen, *Mater. Integr.* **2005**, *18*, 31.
- [60] J. P. Heremans, C. M. Thrush, D. T. Morelli, *J. Appl. Phys.* **2005**, *98*, 63 703.
- [61] J. P. Heremans, C. M. Thrush, D. T. Morelli, *Phys. Rev. B* **2004**, *70*, 115 334.
- [62] W. Kim, J. Zide, A. Gossard, D. Klemov, S. Stemmer, A. Shakouri, A. Majumdar, *Phys. Rev. Lett.* **2006**, *96*, 045 901.
- [63] D. Vashaev, A. Shakouri, *Phys. Rev. Lett.* **2004**, *92*, 106 103.